



Output Limitation Control for 4DOF Magnetic Bearings

Ngoc Hoi Le, Tung Lam Nguyen*, Minh Duc Duong, and Quang Dich Nguyen

Abstract— In the currently-used electrical drive systems, bearings are increasingly widely applied owing to its capability of minimizing friction during operation, allowing rotating shafts to smoothly and easily rotate, as well as suffer from almost no mechanical wear. Recently with the development of control techniques and semiconductor components, magnetic bearings, mainly Active Magnetic Bearing (AMB), gradually substitute original bearings in numerous applications, typical high-speed rotation systems, and high-accuracy-demanding systems. In addition, magnetic bearings result in long life without the use of any lubrication system, thereby eliminating the complexity of lubricant systems and encouraging green operations of rotating systems. Therefore, an appropriate control system is essential for an AMB system to utilize its positive characteristics and improve working efficiency. In this study, based on the Lyapunov Stability, a nonlinear Adaptive Backstepping Controller is applied to the AMB system, so that it is possible to maintain the rotor - a rotating shaft - at equilibrium point during operation. Besides, an exponentially convergent nonlinear observer is also introduced into the system to estimate the unmeasured variables - displacement velocity of the rotating shaft since this is unavailable for measurement and feedback as well. The reliability of all methods applied is verified and confirmed by simulation results.

Keywords— Active magnetic bearing, barrier Lyapunov function, nonlinear observer, backstepping.

1. INTRODUCTION

The requirement of a supporting mechanism replacing conventional mechanical bearings is essential in modern manufacturing industry. Possessing non-contact and non-lubrication properties, an active magnetic bearing (AMB) has been a potential candidate recently [1][2][3]. The pivot problem of magnetic bearing system is to maintain rotor shaft in the face of the nonlinearity in the system. In recent years, various control approaches have been proposed to AMB systems. In [4] and [5], various linear controller structures for AMBs such as PI/PD, PID, LQ, LQ/LTR have been considered. Genetic algorithm is also used for parameter optimization. In order to improve the operational performance of AMB with linear controller structures, Linear Quadratic Gaussian Controller with Extended Kalman Filter is also applied to AMB in [6]. In [7], four degrees of freedom AMB with gyroscopic impacts is considered, and due to the lack of velocity feedback information, the authors employ robust control with rotor position output feedback. In [8], the state feedback controller is proposed to control the AMB. Five explicit sets of stability constraints had been proposed to guarantee the state feedback loop is not over-designed. Adaptive control with nonlinear observer is also used in [9] to overcome the nonlinear and parametric

uncertainties in AMB. In addition, to attenuate the disturbance and increase the robustness to model uncertainties, sliding mode control is applied to control the AMBs in [10] and [11]. In [12], a robust Takagi-Sugeno model based fuzzy control has been proposed to stabilize the AMB system with parameter uncertainties and voltage saturation. To increase the robustness and improve the performance of the AMB system subject to disturbances, a hybrid control scheme including a feedback H_∞ controller and disturbance observer-based control is proposed in [13]. In addition, to reject the influence of moving gimbal effect and parameter variation, feedback linearization and extend state observer are used in [14]. Although various problems have been considered in the aforementioned works, there still some limitations such as the motor shaft is considered as a mass point, or the output limitation has not taken into account.

To overcome the above-mentioned limitation, in this paper, we consider the 4DOF Active Magnetic Bearing in which the motor shaft is not a mass point but a cylindrical shaft. Due to only output feedback is available, an exponentially convergent nonlinear observer is used to estimate unmeasured rotor speed. To guarantee the system stability and keep the rotor shaft of AMBs at the equilibrium point during operation, a nonlinear adaptive controller with backstepping design strategy is introduced. In order to avoid multi-input situation, a current switching scheme is utilized. Moreover, the paper introduces barrier term in Lyapunov candidate function to control system output in a limit which bear a practical meaning since it prevents the rotor from coming into contact with the stator.

This paper is organized as follows. First, in the section 2, the model of 4DOF Active Magnetic Bearing is presented. Then, the nonlinear adaptive controller is

The research is supported by Industrial University of Ho Chi Minh City.

*Ngoc Hoi Le is with Faculty of Electrical Engineering Technology, Industrial University of Ho Chi Minh City.

Tung Lam Nguyen, Minh Duc Duong, and Quang Dich Nguyen are with School of Electrical Engineering, Hanoi University of Science and Technology.

*Corresponding author: Tung Lam Nguyen; Email: lam.nguyentung@hust.edu.vn.

designed using backstepping strategy in Section 3. Simulations is done in Section 4. Finally, Section 5 concludes this paper.

2. SYSTEM MODELLING

Considering a 4DOF Active Magnetic Bearing as in Figure 1, this model can be divided into 2 parts - upper part composed of magnet 1 and 2 while lower counterpart comprising magnet 3 and 4. The upper part includes two identical magnets that are placed opposite to each other, creating two forces (F_1, F_2) of opposite direction. These two forces keep the rotor remained at equilibrium point between two magnets and can be adjusted by adjusting voltage u_1 and u_2 applied to the coils so as to adjust current i_1 and i_2 . Similarly, the lower part includes two identical magnets that are placed opposite to each other, creating two forces (F_3, F_4) of opposite direction. These two forces keep the rotor remained at equilibrium point between two magnets and can be adjusted by adjusting voltage u_3 and u_4 applied to the coils so as to adjust current i_3 and i_4 . It is supposed that the effect rotational motion is negligible, i.e., it is totally decoupled from transverse motions.

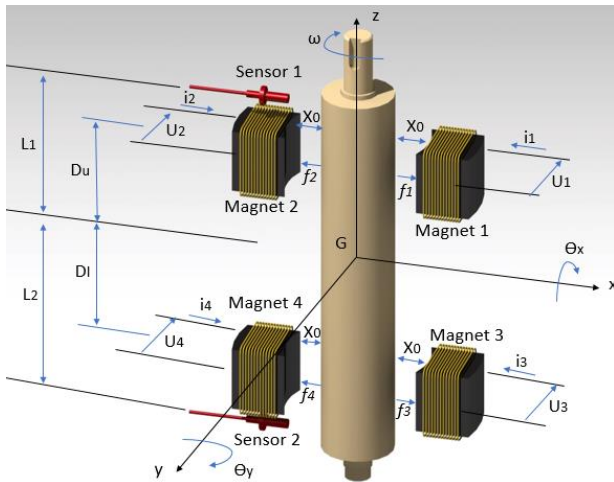


Fig.1. Vertical model of 4-degree-of-freedom AMB.

Now, let's consider the upper part. According to Newton's law:

$$m\ddot{x}_u = F_1 - F_2, \tag{1}$$

where x_u is the displacement of upper part from equilibrium point. Two electromagnetic force F_1 and F_2 can be calculated as [15]:

$$F_1 = \frac{\mu_g N^2 i_1^2 A_g}{4(x_0 - x_u)^2} = \frac{K}{4} \left(\frac{i_1}{x_0 - x_u} \right)^2, \tag{2}$$

$$F_2 = \frac{\mu_g N^2 i_2^2 A_g}{4(x_0 + x_u)^2} = \frac{K}{4} \left(\frac{i_2}{x_0 + x_u} \right)^2, \tag{3}$$

with x_0 is the nominal position of the rotor at equilibrium point, $K = \mu_g N^2 A_g$, μ_g is flux factor of air gap, N is number of coil round, A_g is the cross-section area. It is noted that, the force and current/displacement equation exhibits a nonlinear relationship which causes difficulties

in control design. According to Kirchoff's Voltage Law:

$$u_1 = Ri_1 + L_s \frac{di_1}{dt} + N \frac{d\phi_1}{dt}, \tag{4}$$

$$u_2 = Ri_2 + L_s \frac{di_2}{dt} + N \frac{d\phi_2}{dt}, \tag{5}$$

where R is coil resistor and L_s is coil inductance.

From (1) – (5) we have the equations representing the AMB dynamics for upper part is:

$$\begin{cases} \dot{x}_u = v_u \\ \dot{v}_u = a_u \cdot \left(\frac{i_1}{x_0 - x_u} \right)^2 - a_u \cdot \left(\frac{i_2}{x_0 + x_u} \right)^2 \\ \frac{di_1}{dt} = \frac{2 \cdot (x_0 - x_u)}{2L_s \cdot (x_0 - x_u) + K} \cdot (u_1 - R \cdot i_1 - \frac{K \cdot v_u \cdot i_1}{2 \cdot (x_0 - x_u)^2}) \\ \frac{di_2}{dt} = \frac{2 \cdot (x_0 + x_u)}{2L_s \cdot (x_0 + x_u) + K} \cdot (u_2 - R \cdot i_2 + \frac{K \cdot v_u \cdot i_2}{2 \cdot (x_0 + x_u)^2}) \end{cases} \tag{6}$$

in which $a_u = \frac{K}{4m}$. Similarly, the equations representing the AMB motions for lower part is:

$$\begin{cases} \dot{x}_l = v_l \\ \dot{v}_l = a_l \cdot \left(\frac{i_3}{x_0 - x_l} \right)^2 - a_l \cdot \left(\frac{i_4}{x_0 + x_l} \right)^2 \\ \frac{di_3}{dt} = \frac{2 \cdot (x_0 - x_l)}{2L_s \cdot (x_0 - x_l) + K} \cdot (u_3 - R \cdot i_3 - \frac{K \cdot v_l \cdot i_3}{2 \cdot (x_0 - x_l)^2}) \\ \frac{di_4}{dt} = \frac{2 \cdot (x_0 + x_l)}{2L_s \cdot (x_0 + x_l) + K} \cdot (u_4 - R \cdot i_4 + \frac{K \cdot v_l \cdot i_4}{2 \cdot (x_0 + x_l)^2}) \end{cases} \tag{7}$$

where x_l is the displacement of lower part from equilibrium point, $a_l = \frac{K}{4m}$.

3. CONTROLLER DESIGN

Practically, almost every parameter of AMB system can be measured, and the only exception is velocity. Since the feedback of velocity is needed for controller design, an exponentially convergent nonlinear speed observer [9] is introduced into the system as:

$$\hat{v}_u = \zeta_1 + A_u \xi_1 + k_u x_u, \tag{8}$$

$$\hat{v}_l = \zeta_2 + A_l \xi_2 + k_l x_l, \tag{9}$$

in which $\dot{\zeta}_1 = -k_u \zeta_1 - k_u^2 x_u$, $\dot{\zeta}_2 = -k_l \zeta_2 - k_l^2 x_l$, and

$$\dot{\xi}_1 = -k_u \xi_1 + \frac{i_1^2}{(x_0 - x_u)^2} - \frac{i_2^2}{(x_0 + x_u)^2},$$

$$\dot{\xi}_2 = -k_l \xi_2 + \frac{i_3^2}{(x_0 - x_l)^2} - \frac{i_4^2}{(x_0 + x_l)^2},$$

the initial states $\zeta_u(0) = \zeta_l(0) = 0$, $\xi_u(0) = \xi_l(0) = 0$, and k_u, k_l are positive factors.

Substituting (8) into (6) and (9) into (7), the equations representing the system for the upper part can be rewritten as:

$$\begin{cases} \dot{x}_u = v_u \\ \hat{v}_u = \zeta_1 + A_u \xi_1 + k_u x_u \\ \ddot{x}_u = a_u \left[\frac{i_1^2}{(x_0 - x_u)^2} - \frac{i_2^2}{(x_0 + x_u)^2} \right] \\ \frac{di_1}{dt} = \frac{2 \cdot (x_0 - x_u)}{2L_s \cdot (x_0 - x_u) + K} \cdot (u_1 - R \cdot i_1 - \frac{K \cdot v_u \cdot i_1}{2 \cdot (x_0 - x_u)^2}) \\ \frac{di_2}{dt} = \frac{2 \cdot (x_0 + x_u)}{2L_s \cdot (x_0 + x_u) + K} \cdot (u_2 - R \cdot i_2 - \frac{K \cdot v_u \cdot i_2}{2 \cdot (x_0 + x_u)^2}) \end{cases} \quad (10)$$

And for the lower part

$$\begin{cases} \dot{x}_l = v_l \\ \hat{v}_l = \zeta_2 + A_l \xi_2 + k_l x_l \\ \ddot{x}_l = a_l \left[\frac{i_3^2}{(x_0 - x_l)^2} - \frac{i_4^2}{(x_0 + x_l)^2} \right] \\ \frac{di_3}{dt} = \frac{2 \cdot (x_0 - x_l)}{2L_s \cdot (x_0 - x_l) + K} \cdot (u_3 - R \cdot i_3 - \frac{K \cdot v_l \cdot i_3}{2 \cdot (x_0 - x_l)^2}) \\ \frac{di_4}{dt} = \frac{2 \cdot (x_0 + x_l)}{2L_s \cdot (x_0 + x_l) + K} \cdot (u_4 - R \cdot i_4 - \frac{K \cdot v_l \cdot i_4}{2 \cdot (x_0 + x_l)^2}) \end{cases} \quad (11)$$

Since in this model, two parts of the system are identical to each other, design controller will be designed for one side, and applied similarly to the other counterpart. The system is in of strict feedback form, the control design is based on backstepping strategy as follows.

Considering z_l the displacement between rotor and equilibrium point: $z_l = x_u$. The derivative of z_l can be written:

$$\dot{z}_1 = \dot{x}_u = \zeta_1 + A_u \xi_1 + k_u x_u + \tilde{v}_1 \quad (12)$$

Practically, the displacement needs being limited to a certain extent, or collision between hardware components can make the system collapsed. Therefore, in this paper, Lyapunov stability is used to design the a controller and the Barrier Lyapunov function is applied in order to avoid this incident.

Here, Barrier Lyapunov function V_1 was used:

$$V_1 = \frac{1}{2} \ln \frac{k_b^2}{k_b^2 - z_1^2} + \frac{1}{2k_u d_1} \tilde{v}_1^2 \quad (13)$$

in which k_b is the limitation of displacement ($-k_b \leq z_l \leq k_b$), d_1 is a positive factor, and $\tilde{v}_1 = v_u - \hat{v}_u$. Different from conventional Lyapunov candidate functions taking a form of quadratic of system errors, the logarithm term in V_1 is used to limit z_l in a predefined value k_b [16] and [17].

Taking the derivative of V_1 :

$$\dot{V}_1 = \frac{z_1(\zeta_1 + A_u \xi_1 + k_u x_u + \tilde{v}_1)}{k_b^2 - z_1^2} - \frac{1}{d_1} \tilde{v}_1^2 \quad (14)$$

It is noted that $\dot{\tilde{v}}_1 = \dot{v}_u - \dot{\hat{v}}_u = k_u \tilde{v}_1$.

To achieve $\dot{V}_1 \leq 0$, a virtual controller ξ_{1ctrl} can be chosen as:

$$\xi_{1ctrl} = \frac{1}{A_u} \left[-(k_b^2 - z_1^2) k_1 z_1 - d_1 \frac{z_1}{k_b^2 - z_1^2} - \right. \quad (15)$$

$$\left. k_u x_u - \zeta_1 \right]$$

in which k_1 and d_1 are positive factors. Substituting this into (14), the derivative \dot{V}_1 is obtained as:

$$\dot{V}_1 = -k_1 z_1^2 - d_1 \left[\frac{z_1}{k_b^2 - z_1^2} - \frac{1}{2d_1} \tilde{v}_1 \right]^2 - \frac{3}{4d_1} \tilde{v}_1^2 \leq 0 \quad (16)$$

Here, it is proved that V_l exponentially converges to zero if $\xi_l = \xi_{lctrl}$. Since the global stability condition is not achieved yet, the control design needs expanding to include the error variable z_2 :

$$z_2 = \xi_1 - \xi_{1ctrl} = \xi_1 - \alpha_1. \quad (17)$$

Then,

$$\dot{z}_2 = \dot{\xi}_1 - \frac{\partial \alpha_1}{\partial z_1} (\hat{v}_1 + \tilde{v}_1) - \frac{\partial \alpha_1}{\partial \zeta_1} \cdot \zeta_1 \quad (18)$$

Substituting (17) into (12), the derivative of z_l can be rewritten as:

$$\dot{z}_1 = A_u z_2 - (k_b^2 - z_1^2) k_1 z_1 - d_1 \cdot \frac{z_1}{k_b^2 - z_1^2} + \tilde{v}_1 \quad (19)$$

Considering the Barrier Lyapunov function V_2 :

$$V_2 = V_{1nw} + \frac{1}{2} z_2^2 + \frac{1}{2k_u d_2} \tilde{v}^2 \quad (20)$$

in which d_2 is a positive factor and $\dot{V}_{1nw} = A_u \frac{z_1 z_2}{k_b^2 - z_1^2} + \dot{V}_1$. Taking the derivative of V_2 , it is obtained that:

$$\dot{V}_2 = \dot{V}_1 + A_u \frac{z_1 z_2}{k_b^2 - z_1^2} + z_2 \left(\dot{\xi}_1 - \frac{\partial \alpha_1}{\partial z_1} (\hat{v}_1 + \tilde{v}_1) - \frac{\partial \alpha_1}{\partial \zeta_1} \dot{\zeta}_1 \right) - \frac{1}{d_2} \tilde{v}_1^2 \quad (21)$$

To render $\dot{V}_2 \leq 0$, $\dot{\xi}_1$ is defined as:

$$\dot{\xi}_1 = \alpha_2 = -k_2 z_2 - A_u \frac{z_1}{k_b^2 - z_1^2} - d_2 z_2 \left(\frac{\partial \alpha_1}{\partial z_1} \right)^2 + \frac{\partial \alpha_1}{\partial z_1} \hat{v}_1 + \frac{\partial \alpha_1}{\partial \zeta_1} \dot{\zeta}_1 \quad (22)$$

in which k_2 and d_2 are positive factors. With this control variable, we have

$$\dot{V}_2 = \dot{V}_1 - k_2 z_2^2 - d_2 \left[z_2 \frac{\partial \alpha_1}{\partial z_1} + \frac{1}{2d_2} \tilde{v}_1 \right]^2 - \frac{3}{4d_2} \tilde{v}_1^2 \leq 0 \quad (23)$$

From (8), it is clear that $\dot{\xi}_1$ can be demonstrated as a function of i_1 and i_2 , then $\alpha_2 = \dot{\xi}_1$ can also be demonstrated as:

$$\alpha_2 = \dot{\xi}_1 = -k_u \xi_1 + \frac{i_1^2}{(x_0 - x_u)^2} - \frac{i_2^2}{(x_0 + x_u)^2} \quad (24)$$

Setting $\alpha_u = k_u \xi_1 + \alpha_2$, then,

$$\alpha_u = \frac{i_1^2}{(x_0 - x_u)^2} - \frac{i_2^2}{(x_0 + x_u)^2}. \quad (25)$$

Ultimately, the controlling purpose becomes adjusting the actual current value i stick to the desired current value i_d . As it can be seen, virtual control function $\dot{\xi}_1$ is

defined based on i_l and i_2 - current generated by magnet 1 and magnet 2, respectively. However, letting both currents flowing simultaneously leads to high consumption of electricity, as well as make it difficult to design control function for u_l and u_2 to control the current flowing in both coils. Therefore, in this research, the currents are alternatively switched on and off. To be more specific: when the rotor part is displaced towards magnet 2, i_2 is switched off. Then: $\alpha_u = \frac{i_2^2}{(x_0 - x_u)^2}$, and

$$i_{1d} = (x_0 - x_u)\sqrt{-\alpha_u} \tag{26}$$

Considering z_3 the error variable of i_l and i_{ld} :

$$z_3 = i_l - i_{1d} \tag{27}$$

Taking the derivative:

$$\dot{z}_3 = \frac{2(x_0 - x_u)}{2L_s(x_0 - x_u) + K} \left(-Ri_l - \frac{ki_l}{2(x_0 - x_u)^2} \dot{x}_u + u_l \right) - \frac{di_{1d}}{dt} \tag{28}$$

Setting $A_1 = \frac{2(x_0 - x_u)}{2L_s(x_0 - x_u) + K}$ and $B_1 = -\frac{A_1 ki_l}{2(x_0 - x_u)^2} - \frac{\partial i_{1d}}{\partial z_1}$, equation (28) can be rewritten:

$$\dot{z}_3 = A_1 Ri_l + B_1(\hat{v}_1 + \tilde{v}_1) + A_1 u_l - \frac{\partial i_{1d}}{\partial \xi_1} \dot{\xi}_1 - \frac{\partial i_{1d}}{\partial \zeta_1} \dot{\zeta}_1 \tag{29}$$

Considering the Lyapunov candidate function:

$$V_3 = V_2 + \frac{1}{2} z_3^2 + \frac{1}{2k_u d_3} \tilde{v}_1^2, \tag{30}$$

in which d_3 is a positive factor. Derivative of V_3 is obtained as:

$$\dot{V}_3 = \dot{V}_2 + z_3 \left[-A_1 Ri_l + B_1(\hat{v}_1 + \tilde{v}_1) + A_1 u_l - \frac{\partial i_{1d}}{\partial \xi_1} \dot{\xi}_1 - \frac{\partial i_{1d}}{\partial \zeta_1} \dot{\zeta}_1 \right] - \frac{1}{d_3} \tilde{v}_1^2 \tag{31}$$

At this point, to make $\dot{V}_3 \leq 0$, the control function for u_l can be defined as:

$$u_l = \frac{1}{A_1} \left[A_1 Ri_l - B_1 \hat{v}_1 - k_3 z_3 - d_3 z_3 B_1^2 + \frac{\partial i_{1d}}{\partial \xi_1} \dot{\xi}_1 + \frac{\partial i_{1d}}{\partial \zeta_1} \dot{\zeta}_1 \right] \tag{32}$$

in which k_3 and d_3 are positive constants. Substituting (32) into (31), we can achieve:

$$\dot{V}_3 = \dot{V}_2 - k_3 z_3^2 - d_3 \left[z_3 B_1 - \frac{1}{2d_3} \tilde{v}_1 \right]^2 - \frac{3}{4d_3} \tilde{v}_1^2 \leq 0 \tag{33}$$

When the rotor part is displaced towards magnet 1, i_l is switched off, then $\alpha_u = -\frac{i_2^2}{(x_0 + x_u)^2}$

Control function for u_2 is obtained as:

$$u_2 = \frac{1}{A_2} \left[A_2 Ri_2 - B_2 \hat{v}_1 - k_4 z_4 - d_4 z_4 B_2^2 + \frac{\partial i_{2d}}{\partial \xi_1} \dot{\xi}_1 + \frac{\partial i_{2d}}{\partial \zeta_1} \dot{\zeta}_1 \right] \tag{34}$$

in which k_4 and d_4 are positive factors, and

$$z_4 = i_2 - i_{2d} = i_2 - (x_0 + x_u)\sqrt{-\alpha_u}. \tag{35}$$

Here the design procedure for upper part of rotor is completed. To design controller for the lower one, it is possible to identically follow the steps for the upper, and finally obtain:

$$u_3 = \frac{1}{A_3} \left[A_3 Ri_3 - B_3 \hat{v}_2 - k_7 z_7 - d_7 z_7 B_3^2 + \frac{\partial i_{3d}}{\partial \xi_2} \dot{\xi}_2 + \frac{\partial i_{3d}}{\partial \zeta_2} \dot{\zeta}_2 \right] \tag{36}$$

$$u_4 = \frac{1}{A_4} \left[A_4 Ri_4 - B_4 \hat{v}_2 - k_8 z_8 - d_8 z_8 B_4^2 + \frac{\partial i_{4d}}{\partial \xi_2} \dot{\xi}_2 + \frac{\partial i_{4d}}{\partial \zeta_2} \dot{\zeta}_2 \right] \tag{37}$$

4. SIMULATIONS

With the acquired the AMB equations of motion and control, a simulation model is constructed to assess the stability and reliability of the controller for a 4-DOF AMB system. Parameters of the system as below:

Table 1. System's parameters for simulations

Parameter	Symbol	Value
Rotor weight	m	5kg
Coil rounds	N	400 rounds
Nominal air gap	x_0	0.004m
Displacement limit	k_b	0.001m
Initial position of rotor upper part	x_u	0.0004m
Initial position of rotor lower part	x_l	0.0004m
Coil inductance	L_s	0.001H
Cross-section area	A_g	0.001m
Air gap factor	μ_g	1.256×10^{-6}
Inertia	I_r	$2.90 \times 10^{-2} \text{ kgm}^2$
Distance from shaft center to upper magnet	D_u	$4.166 \times 10^{-2} \text{ m}$
Distance from shaft center to lower magnet	D_l	$7.602 \times 10^{-2} \text{ m}$

Control gains are selected as below:

- For the upper part: $k_1=75$; $k_2=250$; $k_3=160$; $k_4=160$; $d_1=9.5 \times 10^{-6}$; $d_2=10^{-10}$; $d_3=3 \times 10^{-15}$; $d_4=3 \times 10^{-15}$; $k_u=7.75$.

- For the lower part: $k_5=65$; $k_6=300$; $k_7=180$; $k_8=180$; $d_5=9 \times 10^{-6}$; $d_6=5 \times 10^{-10}$; $d_7=4 \times 10^{-15}$; $d_8=4 \times 10^{-15}$; $k_l=5$.

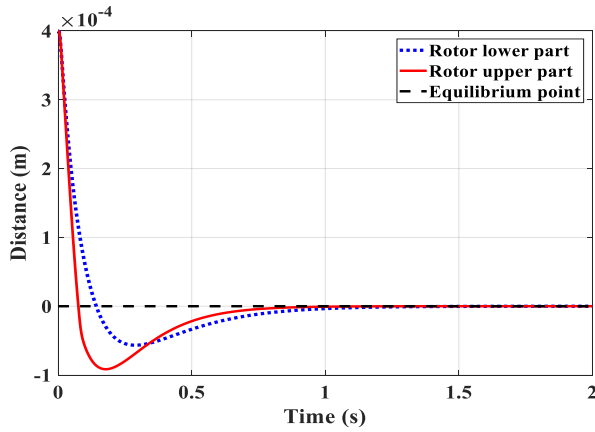


Fig. 2. Rotor displacement.

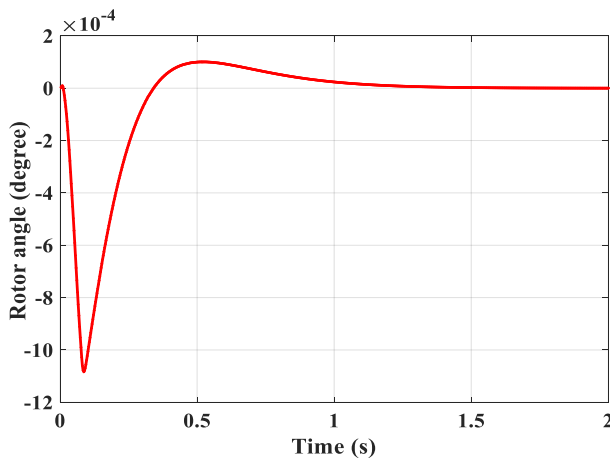


Fig. 3. Rotor angle.

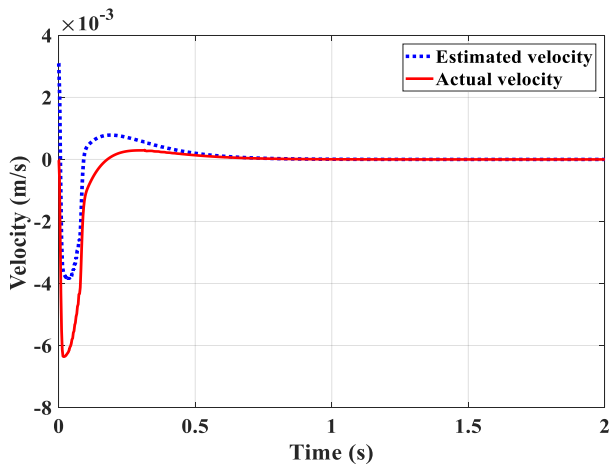


Fig. 4. Upper rotor displacement velocity.

At the initial condition, the AMB rotor is attached to one side of the stator and then the control is activated to drive the rotor to the center of the two stators. Fig. 2 shows that after 1s, the control successfully steers the rotor to zero position, consequently the rotor angle also reaches zero degree. The effectiveness of introducing barrier term in selection of the Lyapunov is presented in Fig. 1 where the displacement overshoot is limited below the nominal airgap ($k_b=0.004$). Fig. 4 and 5 indicatives

that the estimated speed closely track the actual values. Electrical signals in the AMB in Fig. 6, 7, 8, and 9 clearly demonstrate complementarily switching nature of two opposite magnets. In addition, the control input voltage is practical for the AMB under consideration.

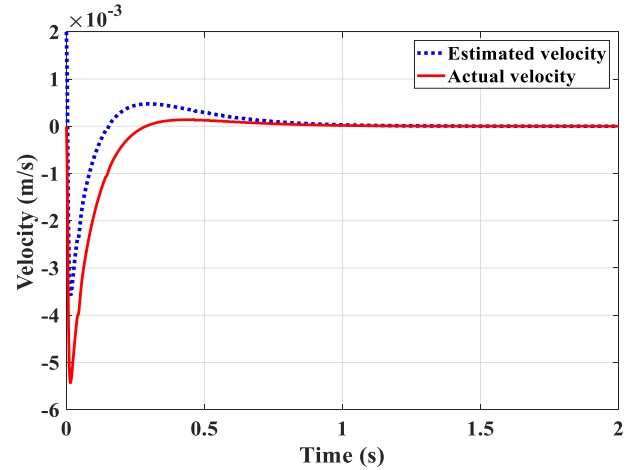


Fig. 5. Lower rotor displacement velocity.

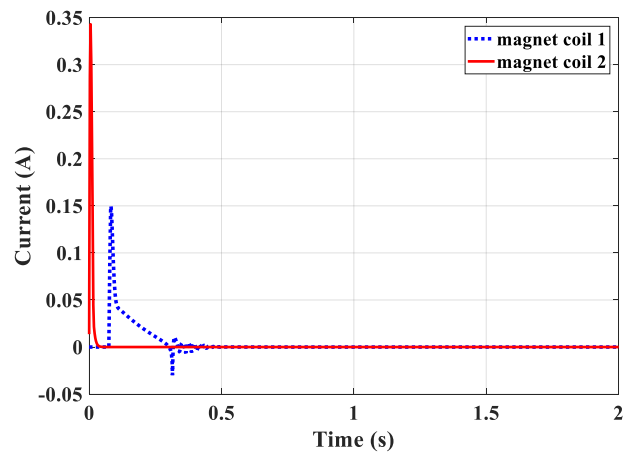


Fig. 6. Upper rotor currents in magnet coils.

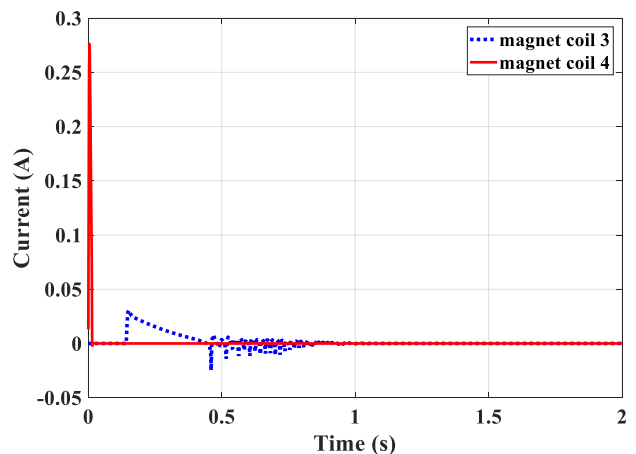


Fig. 7. Lower rotor currents in magnet coils.

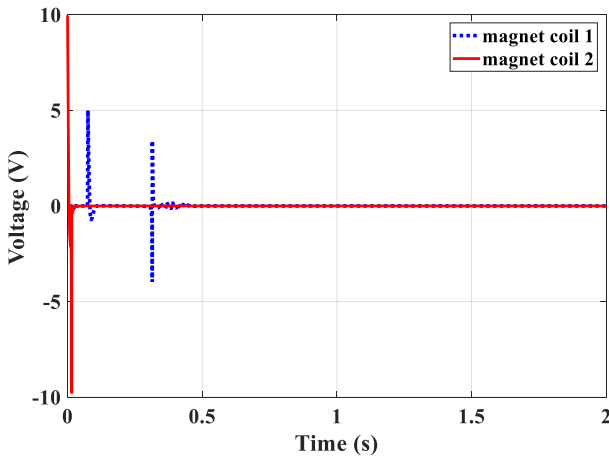


Fig. 8. Upper rotor voltages applied to magnet coils.

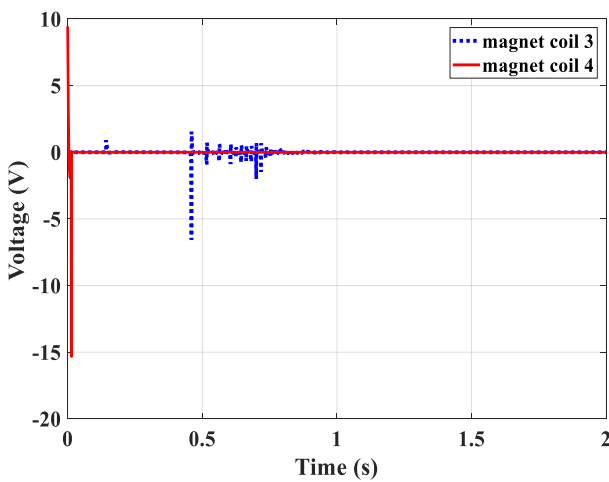


Fig. 9. Lower rotor voltage applied to magnet coils.

5. CONCLUSIONS AND FUTURE WORKS

This study introduces the procedures in designing a nonlinear controller based on the Backstepping method and with the use of Barrier Lyapunov function for Active Magnetic Bearings (AMB). With the feedback of rotor displacement, current and voltage of the magnets, as well as estimated velocity of displacement, the controller succeeds in not only maintaining the shaft at equilibrium point but also restricting movement range during initiation. As can be seen in the simulation results, the usage of the Lyapunov method leads to the effectiveness and robustness of the control system, hence the stability of the AMB system. Besides, the convergent nonlinear observer introduced is proved to bring high-accuracy estimation of velocity, allowing us to overcome the difficulties of unknown parameters in the system. Experimental results are found satisfactory and promising for the active magnetic bearing system.

Nevertheless, there still stand some shortcomings within this study. One is, the controller factors significantly affect the outcomes of the controller, and even minor changes in these factors can lead to completely different results. Therefore, a clear study to discover and tune these coefficients should be found, or else this process is conducted without basing on any basis, hence taking a considerable amount of time.

Certain methods such as genetic algorithm or particle swarm might be the potential to handle this difficulty. Another point is that AMB system, as well as the backstepping method, stands a great chance of being applied widely in the real world, meaning that its reliability should be ensured as much as possible. Therefore, some ignored conditions, such as power loss or environmental affection, can be taken into consideration to make the entire system more practical and applicable.

REFERENCES

- [1] H. Y. Kim and C. W. Lee (2006). Design and control of active magnetic bearing system with Lorentz force-type axial actuator. *Mechatronics*, vol. 16, no. 1, pp. 13–20, 2006.
- [2] C. W. Lee and H. S. Jeong (1996). Dynamic modeling and optimal control of cone-shaped active magnetic bearing systems. *Control Eng. Pract.*, vol. 4, no. 10, pp. 1393–1403, 1996.
- [3] A. Pilat (2010). Analytical modeling of active magnetic bearing geometry. *Appl. Math. Model.*, vol. 34, no. 12, pp. 3805–3816, 2010.
- [4] R. P. Jastrzębski and R. Pöllänen (2009). Centralized optimal position control for active magnetic bearings: Comparison with decentralized control. *Electrical Engineering*, vol. 91, no. 2, pp. 101–114, 2009.
- [5] M. Puskaric, Z. Car, and N. Bulic (2018). Magnetic bearing control system based on PI and PID controllers. *Teh. Vjesn.*, vol. 25, no. 1, pp. 136–140, 2018.
- [6] V. Janardhanan and S. S. Mathew (2015). Improvement of Operational Performance of Active Magnetic Bearing using Nonlinear LQG Controller. *vol. 4, no. 07*, pp. 1187–1192, 2015.
- [7] Y. X. Yan and G. R. Duan (2006). Robust control of magnetic bearing with gyroscopic effects using output feedback controller. *1st Int. Symp. Syst. Control Aerosp. Astronaut.*, vol. 2006, pp. 778–782, 2006.
- [8] N. C. Tsai, B. Y. Wu, and S. L. Hsu (2007). Stability constraints of active magnetic bearing control systems. *Int. J. Control*, vol. 80, no. 12, pp. 1893–1902, 2007.
- [9] S. Sivrioglu (2007). Adaptive control of nonlinear zero-bias current magnetic bearing system. *Nonlinear Dyn.*, vol. 48, no. 1–2, pp. 175–184, 2007.
- [10] M. S. Kang, J. Lyou, and J. K. Lee (2010). Sliding mode control for an active magnetic bearing system subject to base motion. *Mechatronics*, vol. 20, no. 1, pp. 171–178, 2010.
- [11] J. F. Mao, A. H. Wu, G. Q. Wu, and X. D. Zhang (2011). Sliding Mode Control of Magnetic Bearing System Based on Variable Rate Reaching Law. *Key Eng. Mater.*, vol. 460–461, pp. 827–830, 2011.
- [12] H. Du, N. Zhang, J. C. Ji, and W. Gao (2010). Robust fuzzy control of an active magnetic bearing subject to voltage saturation. *IEEE Trans. Control Syst. Technol.*, vol. 18, no. 1, pp. 164–169, 2010.

- [13] A. Noshadi, J. Shi, W. S. Lee, P. Shi, and A. Kalam (2017). Robust control of an active magnetic bearing system using H_∞ and disturbance observer-based control. *J. Vib. Control*, vol. 23, no. 11, pp. 1857–1870, 2017.
- [14] C. Liu, G. Liu, and J. Fang (2017). Feedback Linearization and Extended State Observer-Based Control for Rotor-AMBs System with Mismatched Uncertainties. *IEEE Trans. Ind. Electron.*, vol. 64, no. 2, pp. 1313–1322, 2017.
- [15] D. H. Nguyen, T. L. Nguyen, M. L. Nguyen, and H. P. Nguyen (2019). Nonlinear Control of an Active Magnetic Bearing with Output Constraint. *Int. J. Electr. Comput. Eng.*, vol. 8, no. 5, p. 3666, 2019.
- [16] Y. Wu and J. Yao (2017). Barrier Lyapunov function-based adaptive output feedback failure compensation for a class of non-linear systems with unknown dead-zone non-linearity. *Trans. Inst. Meas. Control*, vol. 39, no. 8, pp. 1169–1181, 2017.
- [17] Z. L. Tang, K. P. Tee, and W. He (2013). Tangent barrier Lyapunov functions for the control of output-constrained nonlinear systems. *IFAC Proc. Vol.*, vol. 3, no. PART 1, pp. 449–455, 2013.